Use of ARM/NSA Data to Validate and Improve the Remote Sensing Retrieval of Cloud and Surface Properties in the Arctic from AVHRR Data

X. Xiong
QSS Group, Inc.
National Oceanic and Atmospheric Administration
National Environmental Satellite, Data, and Information Service
Office of Research and Applications
Camp Springs, Maryland

R. Storvold and C. Marty
Geophysical Institute
University of Alaska
Fairbanks, Alaska

K. H. Stamnes
Stevens Institute of Technology
Hoboken, New Jersey

B. D. Zak
Sandia National Laboratories
Albuquerque, New Mexico

Introduction

Clouds in the Arctic have an important impact on the radiative energy balance. However, the effects of clouds still constitute one of the largest uncertainties in the study of climate change. Because the surface observations are limited, especially in the polar regions, satellite remote sensing which has proven useful for deriving some cloud properties, such as cloud fraction, optical depth, effective droplet size, and liquid water path (LWP), will be necessary. The availability of more than 20 years of advanced very high resolution radiometer (AVHRR) data covering the Arctic makes this particular satellite dataset valuable for the retrieval of cloud properties for climatological studies.

Cloud discrimination from satellite data is difficult in the Arctic due to the small contrast in both visible and infrared channels between clouds and the underlying snow or ice surfaces. In addition, current satellite sensors are operating near the limit of their performance range. Frequent isothermal conditions or temperature inversions occurring in the lower troposphere and large bidirectional reflectance effects in the polar make cloud discrimination much more difficult in the polar regions than at lower latitudes. The largest discrepancies in cloud fraction among different satellite climatological studies are found in the Polar Regions. Uncertainty in cloud discriminations from snow/ice surfaces has hindered our ability

to get accurate albedo and surface temperature, and further retrieve cloud optical properties. Higher albedo and/or large bidirectional reflectance effects over snow/ice surfaces at large SZAs makes the retrieval of cloud properties in the Arctic different from that in mid-to-lower latitude regions.

To improve our capacity to use AVHRR data to study the cloud climatology in the Arctic, our efforts begins from the improvement of cloud discrimination from snow/ice surfaces, retrieval of ground albedo, temperature, to the improvement of cloud retrievals. A flow chart of the processing of AVHRR data is shown in Figure 1. A series of model simulations have been made for the design of these algorithms. Validation of these algorithms has been made using ground-based observations during the Surface Heat and Energy Budget of the Arctic (SHEBA) project and the on-going observations at the North Slope of Alaska (NSA) through the Atmospheric Radiation Measurement (ARM) Program. We present some of our work regarding the improvements on the retrieval of cloud and surface properties and the comparison of some satellite-derived products with surface observations.

Cloud Discrimination from Snow/Ice Surfaces in the Arctic

Considerable efforts aimed at cloud detection and classification, for example in the International Satellite Cloud Climatology Program (ISCCP), AVHRR Processing scheme Over Land, cLoud and Ocean (APOLLO), and the National Oceanic and Atmospheric Administration (NOAA) cloud advanced very high resolution radiometer (CLAVR) algorithms, have led to reliable cloud masks applicable at low and mid latitudes. The techniques used range from the most simple threshold tests, or bi-spectral threshold tests using only spectral information, to more complicated techniques using both spectral and textural features, such as pattern recognition, fuzzy logic, and neural network approaches applied to groups of pixels in an image.

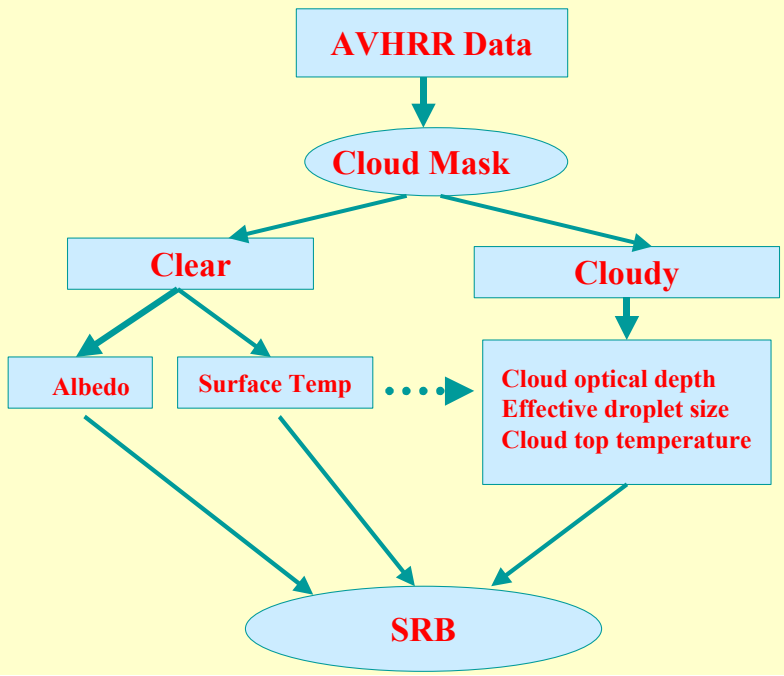

Figure 1. Flow chart of AVHRR data processing in the Arctic.

Most of these techniques for cloud discrimination are based primarily on visible and infrared data and do not work over snow/ice surfaces. The much higher reflectance near 3.75 μm over liquid water clouds than over snow/ice surfaces, results in a significant increase of the brightness temperature in channel 3 (BT3). Therefore, the brightness temperature difference between AVHRR channels 3 and 4 (BTD34 = BT3 BT4) becomes much larger for cloudy than for clear-sky conditions. For this reason, BTD34 has been widely used for cloud detection over snow and ice surfaces. However, the contribution of reflected solar radiation to BT3 depends strongly on the solar zenith angle (SZA) and the bidirectional reflectance of clouds. This makes the choice of threshold difficult, and use of a uniform threshold is inaccurate. Use of normalized reflectances in channel 3 (R_3) may give better results, but they were observed to vary substantially even across a single scan line over snow or ice. Therefore, we use top of the atmosphere (TOA) albedo in the 3.75-μm channel, r_3, which depends only on SZA, for cloud discrimination. In the derivation of the reflected solar radiation at the TOA, AVHRR channel 4 is used to remove the thermal component in channel 3 approximately. Anisotropic correction to the normalized reflectance R_3 is made by dividing an anisotropic correction factor (ARF), which is obtained from rigorous radiative transfer simulations and saved in look-up tables. The simulated ARFs are consistent with those derived from the Nimbus 7 ERB (Earth Radiation Budget) and geostationary operational environmental satellite (GOES) data (Suttles et al. 1988) (Figure 2). As R_3 depends on the cloud top temperature, or BT4 over a thick liquid water cloud, temperature correction to R_3 is required (Figure 3) before we used an empirical threshold function, which only depends on SZA.

Because the magnitude of r_3 over thin clouds and/or ice clouds is small, use of r_3 to discriminate thin and/or ice clouds from snow/ice surfaces is difficult. We therefore employ the brightness temperature difference between channels 4 and 5 (BTD45) to detect thin clouds or ice clouds. This cloud discrimination algorithm is applied to daytime AVHRR data obtained between May and August 1998 over the SHEBA ice camp deployed in the Arctic Ocean and at the ARM NSA site in Barrow, Alaska. We find that the AVHRR-derived cloud cover fractions are a good agreement with the surface observations obtained at SHEBA and at ARM NSA site as shown in Figures 4 and Figure 5.

Retrieval of Surface Albedo and Surface Temperature from AVHRR

Surface albedo is one of the most important factors influencing the radiation budget of the earth-atmosphere. Of all the surface types on earth, snow and ice surfaces have the highest albedo. The bidirectional reflectance over snow or ice surfaces is pronounced for the large SZAs encountered in the Arctic. Thus, accurate determination of the albedo and the bidirectional reflectance distribution function (BRDF) is essential for reliable estimation of the radiation budget in the Arctic, and for the derivation of cloud properties as well.

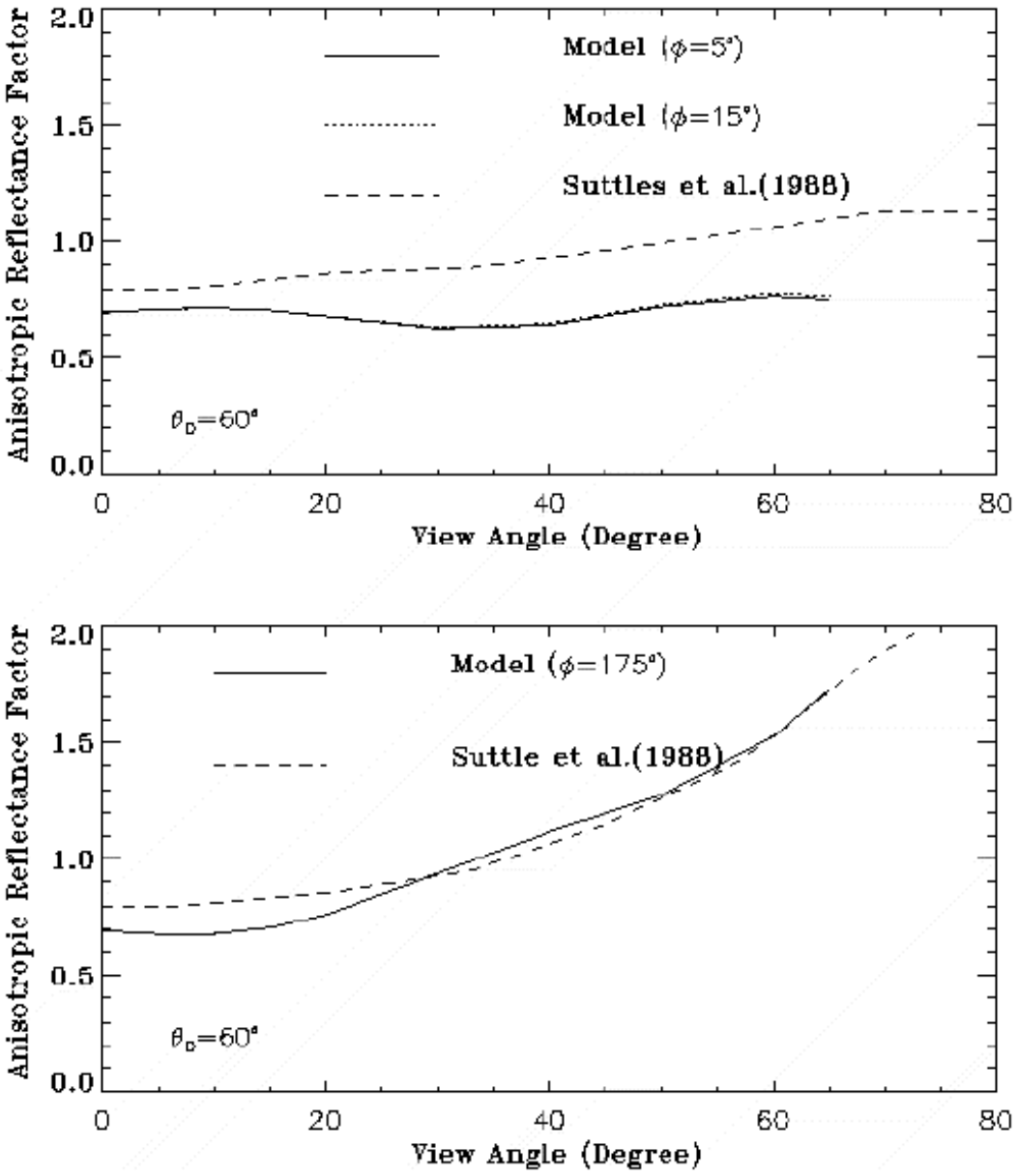

Figure 2. Comparison of model-simulated anisotropic correction factors with that from Suttles et al. (1999).

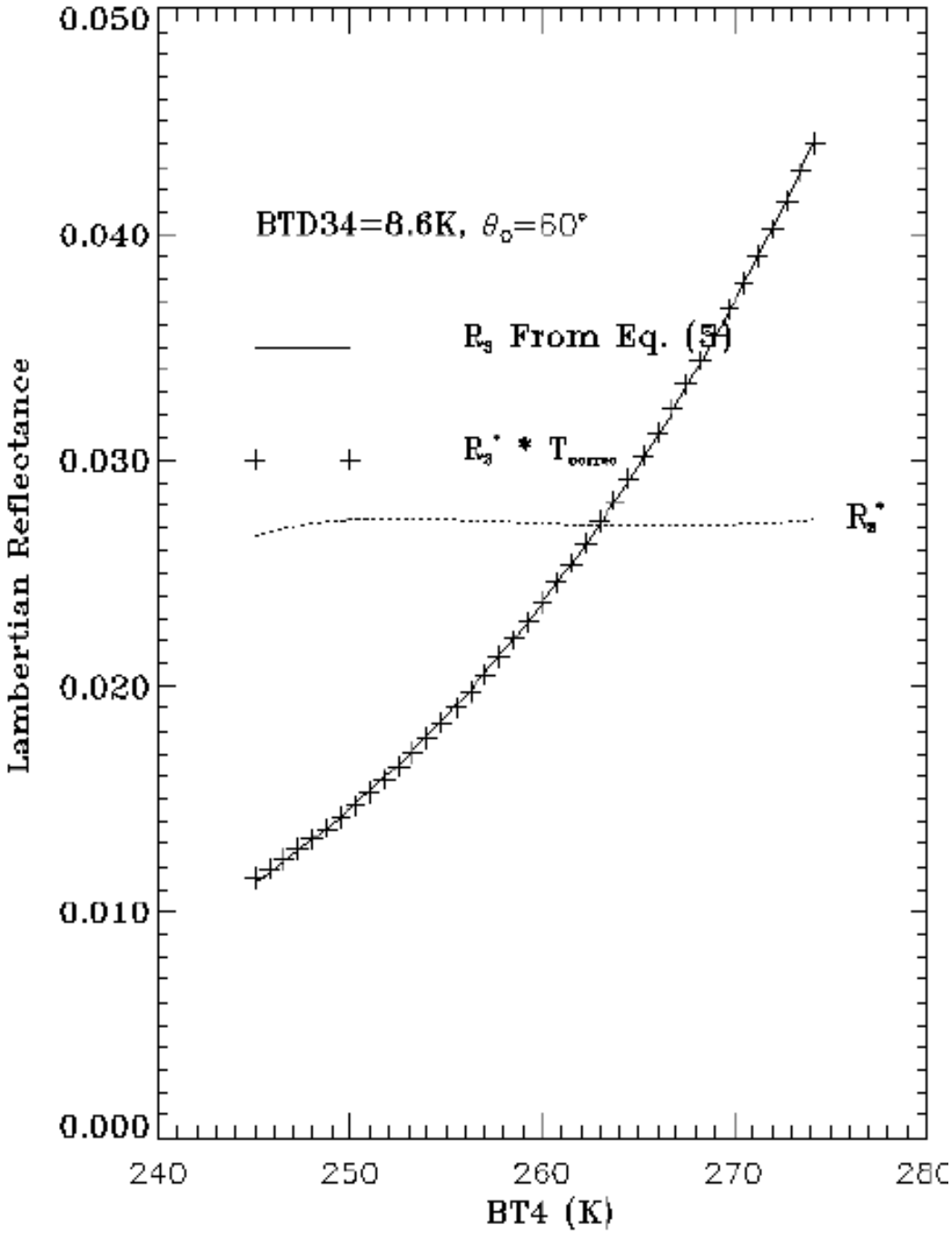

Figure 3. Dependence of normalized reflectance in channel 3 with the cloud top temperature BT4 over thick clouds before and after temperature correction.

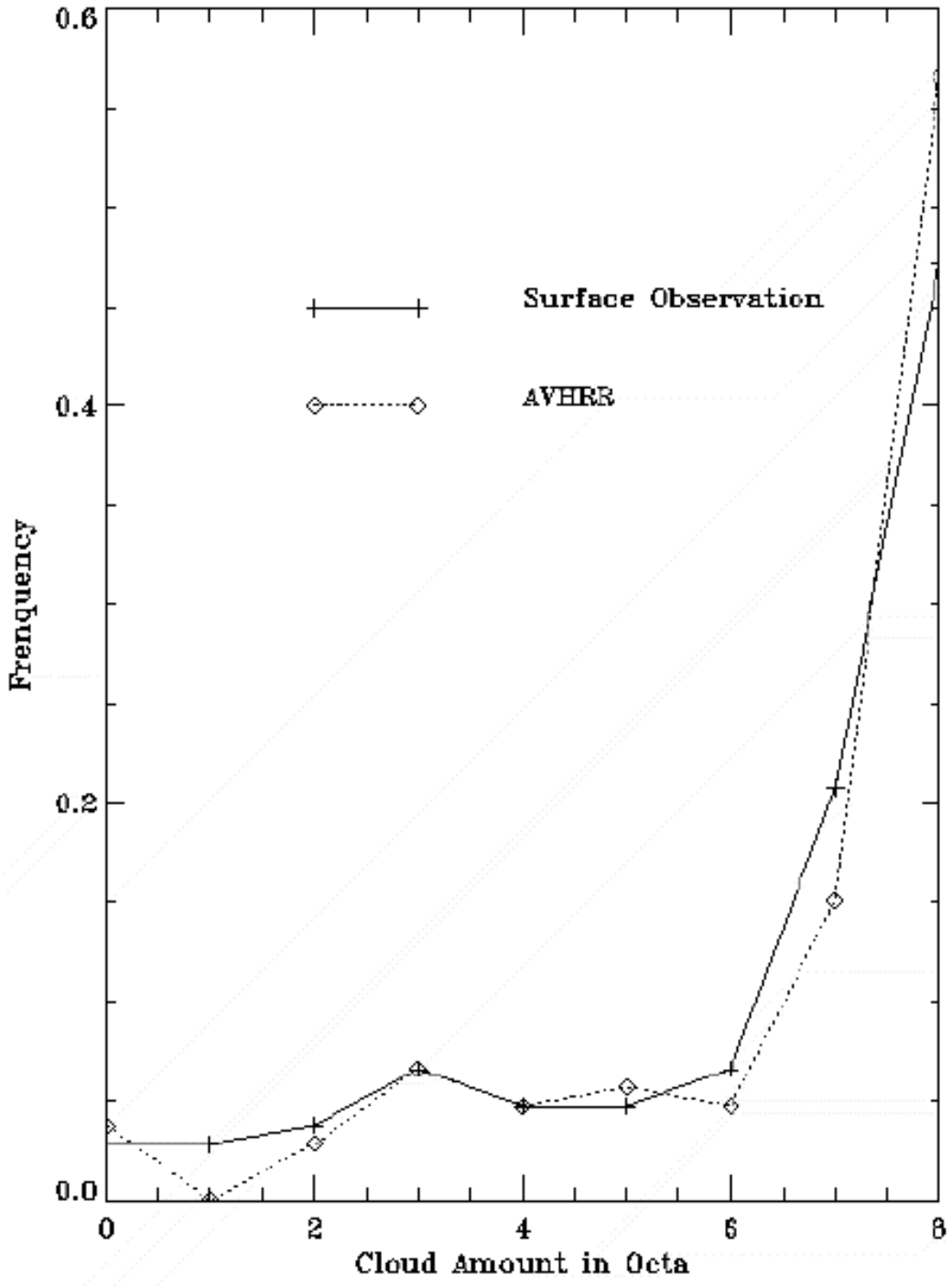

Figure 4. Frequency distribution of cloud cover fraction derived from AVHRR and from surface observations during SHEBA from April to August 1998.

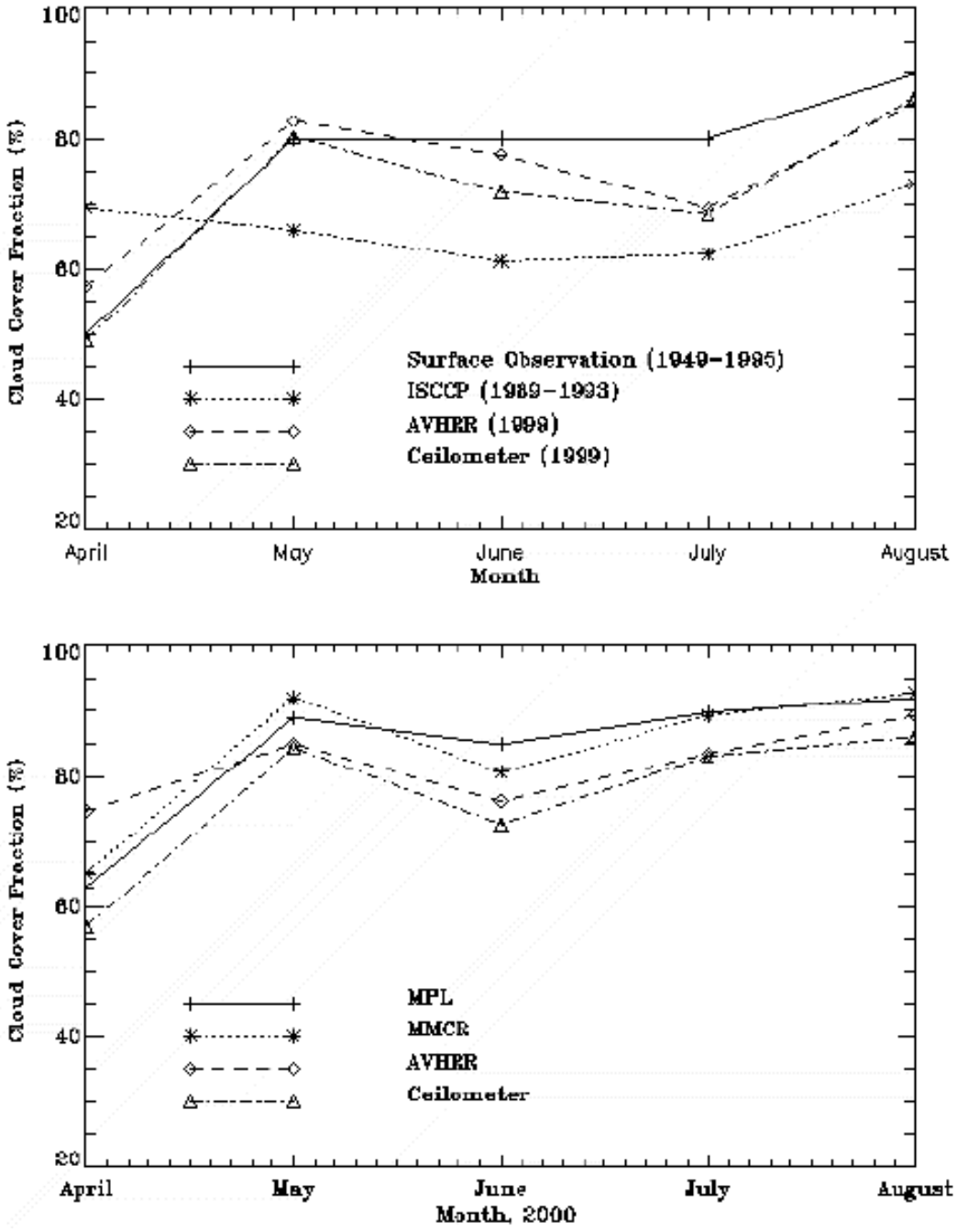

Figure 5. Comparison of cloud cover fraction from AVHRR and from surface observations at the ARM NSA in 1999 and 2000.

An algorithm based on look-up tables is used to retrieve narrowband albedo for AVHRR channels 1 and 2. These values of "albedo" are obviously a function of satellite-viewing geometry, so an anisotropic correction is required to derive the "albedo" that is not related to the satellite viewing geometry. Anisotropic correction factors are obtained from rigorous radiative transfer simulations, in which the snow and ice surface is treated as an additional layer combined with different layers of atmosphere.

Narrow-to-Broadband-Conversion (NTBC) is required to derive the broadband albedo widely used in climate models. The continuous solar illumination during the summer results in a rapid change of the surface physical conditions, such as the melting of snow and ice, and the formation of ponds and lakes. This season between May and August in the Arctic is characterized by rapid change of surface physical conditions, called the "Transition Season," and rapid change of surface albedo. It is found that the NTBC depends on the melting conditions of snow/ice as shown in Table 1. A NTBC scheme based on a rigorous radiative transfer model and surface measurements, is used to derive the broadband albedo. Figure 6 shows a preliminary result for the comparison of albdeo derived from AVHRR with that from surface observation at NSA.

Table 1. Narrow-to-broadband conversion (NTBC) over snow/ice surfaces.

Source	NTBC	Surface Type
Lindsay and Rothrock (1994)	$\alpha = 0.43\alpha_1 + 0.47\alpha_2$	Antarctic snow
Stroeve et al. (1997)	$\alpha = 0.04123.43 + 0.655\alpha_1 + 0.216\alpha_2$	Greenland Ice Sheet
Xiong et al. (2002)	$\alpha = 0.007+ 0.542\alpha_1 + 0.34\alpha_2$	SHEBA Data
Xiong et al. (2002)	$\alpha = -0.009 + 0.28(1+8.26\gamma)\ \alpha_1 + 0.63(1-3.96\gamma)\alpha_2$ $\gamma = (\alpha_1 - \alpha_2) / (\alpha_1 + \alpha_2)$	SHEBA Data

Retrieval of Cloud Optical Depth, Effective Droplet Size and Cloud Top Temperature from AVHRR

Many studies have been conducted to determine cloud optical depth τ and effective particle radius (r_e) from the reflected solar radiation in the visible and near-infrared (NIR) spectral range, but most of them were done over low albedo surfaces. Most of these algorithms rely on the fact that the reflectance of clouds in a nonabsorbing channel in the visible wavelength region is primarily a function of cloud optical depth, whereas the reflectance in a water-absorbing channel in the NIR is primarily a function of cloud droplet size. However, in the Polar Regions, the surface is covered by snow/ice most of the time throughout the year, and visible solar radiation in AVHRR channel 1 (0.58-0.68 μm) reflected by clouds over a bright snow/ice surface is not as sensitive to the cloud optical depth as over a dark surface. So, it is difficult to use AVHRR channel 1 for the retrieval of τ over snow/ice surfaces. Because the reflectance in channel 2 (0.725-1.10 μm) is more sensitive to the cloud optical depth over snow/ice surfaces, in our retrieval AVHRR channels 2, 3, and 4 are used to retrieve the cloud depth, effective droplet size, and cloud top temperature simultaneously.

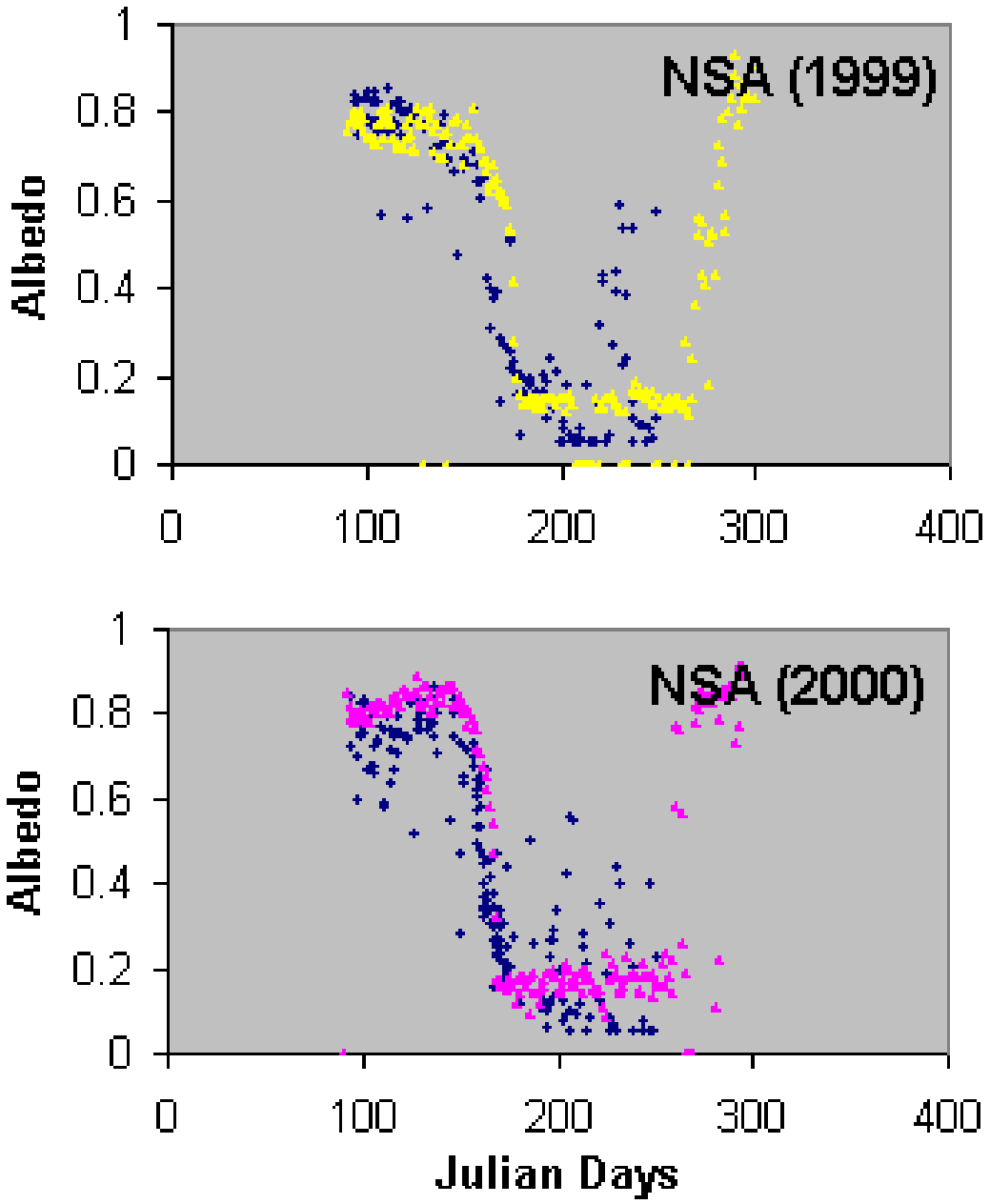

Figure 6. Comparison of AVHRR-derived albedo (yellow or pink color) with surface observations (blue color) at the NSA site in 1999 and 2000.

Difference of AVHRR-Derived Cloud Optical Depth with that Derived from Surface Measurements of Solar Irradiance

To further validate the use of AVHRR data to retrieve cloud properties, we processed more than 100 overpasses of AVHRR data collocated with the SHEBA data during the melt season of 1998. In our retrievals the surface is taken to be new snow with snow grain size of 200 mm between April 15 and May 19. Between May 20 and June 9, we fix the snow grain size at 1000 μm. After June 10 the surface is treated as a Lambertian reflector, and we adopt albedo-values from the SHEBA measurements reported by Perovich et al. (1999). Comparison of the satellite-retrieved cloud optical depth and the cloud optical depth retrieved from coordinated downward solar irradiances measured at SHEBA (Figure 7) shows that between April 15 and May 30, the satellite-retrieved mean cloud optical depth τ_{sat} is 2.3 times of τ_{surf} before the end of May, while after June 1, τ_{sat} is only 19.3% larger than τ_{surf}. If we used the average of the radiance for a domain of 30*30 pixels over the SHEBA ice camp for the retrieval. The retrieved τ_{sat} before June 1 is now 2.5 times of τ_{surf} and after 1 June, τ_{sat} is 15.2% higher than τ_{surf} (Xiong et al. 2002).

Possible Reasons for the Overestimate of Cloud Optical Depth from AVHRR

The sources of uncertainties in the satellite retrieval of cloud properties mainly include (1) errors in satellite-measured radiance (i.e., measurement noise and calibration error), and (2) errors related to the use of a homogeneous cloud layer in a plane-parallel radiative transfer model, like (a) fractional cloud cover, (b) overlap of cirrus over low water cloud, and (c) inhomogeneous cloud stratification, and (3) the specification of the lower boundary conditions, i.e., surface albedo and surface temperature.

To find out the reasons for the overestimate of cloud optical depth in the Arctic spring, we first examined the effect of cloud vertical stratification on satellite remote sensing of cloud properties from AVHRR in the Arctic. The vertically inhomogeneous cloud stratification is considered by dividing the cloud into five layers with r_e increasing from cloud bottom to top according to the model of Stephens and Platt (1987). Figure 8 shows the relative error of the derived cloud optical depth to the true optical depth as a function of r_e (top) for cloud t = 4, 15 and 30. These results demonstrate that the satellite-derived τ is overestimated by 5% to 20%, and the error is larger for clouds with a larger cloud effective droplet size.

The lower panel in Figure 8 shows the retrieved effective droplet radius compared to the value at cloud top as a function of τ for cloud top r_e = 5 and 15 μm in inhomogeneous clouds. The retrieved r_e is 10% to 20% lower than the r_e at the top of the cloud.

For cirrus overlapping liquid water clouds, the reflectances in channels 2 and 3 is smaller than that over liquid water clouds, so the retrieved optical depth will be underestimated.

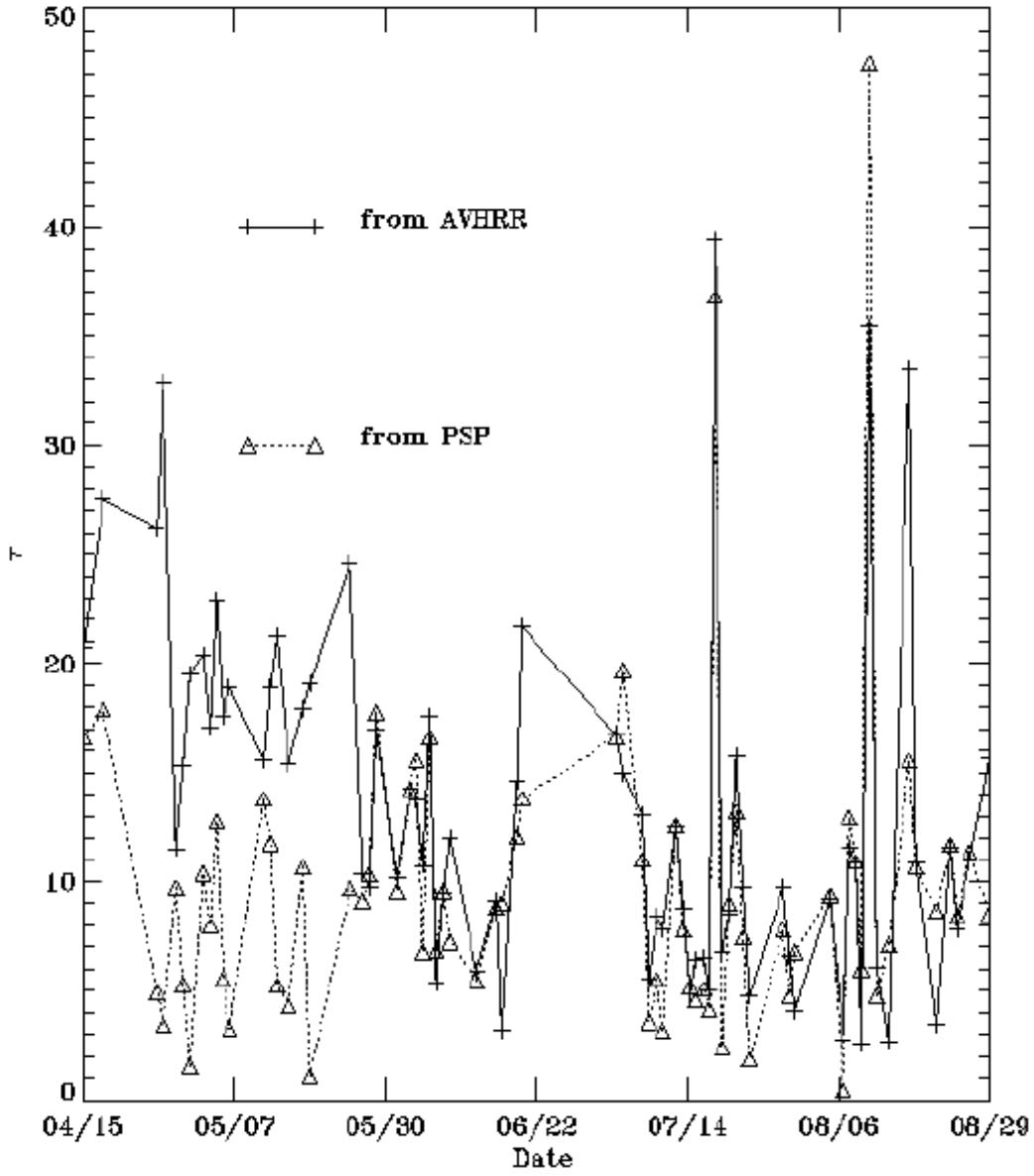

Figure 7. Comparison of AVHRR derived cloud optical depth with that derived from surface-measured solar irradiance during the SHEBA project.

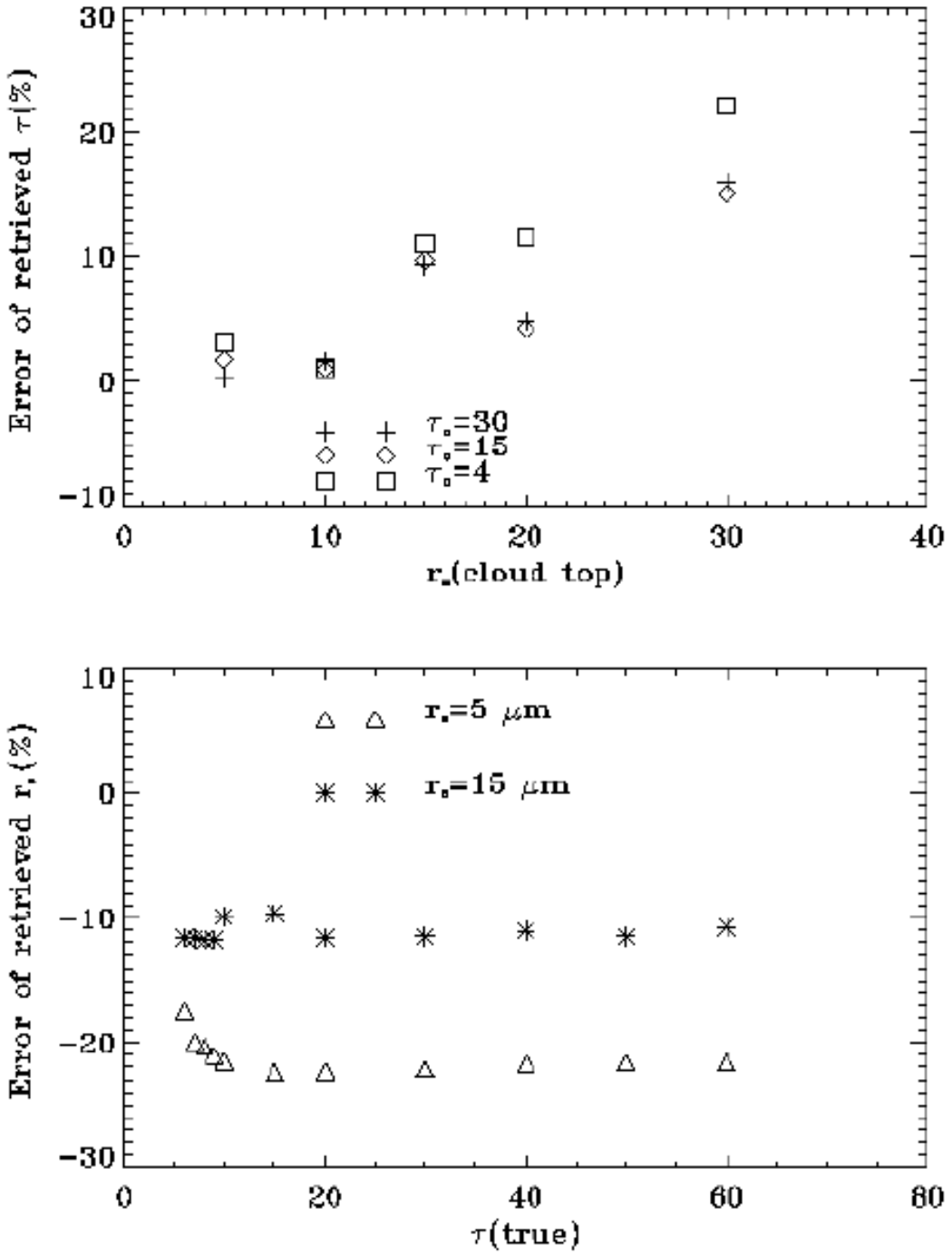

Figure 8. Relative error of cloud optical depth and effective droplet size for inhomogeneous clouds.

Since the spatial resolution for AVHRR is at best 1.1 km (nadir), the pixel may be partly cloud covered. So, we need to test the impact of a misidentification of partly cloudy pixels as overcast on the retrieval of cloud optical depth and effective droplet radius, and the resulting uncertainty in the estimation of the radiation budget.

Radiation field for a partial or broken cloud is complicated. A simple model is used in which the radiance and flux is a linear function of cloud cover fraction:

$$DSSR = DSSR_{cld} * r + DSSR_{clr} * (1 - r) \quad (1)$$

$$R = R_{cld} * r + R_{clr} * (1 - r) \quad (2)$$

Where r is the cloud cover fraction. Figure 9 shows the variation of retrieved cloud optical depth and the effective droplet radius for broken cloud cover with r varying between 0.25 and 1.0. The errors in the retrieved cloud optical depth and effective droplet size for cloud cover fractions of 0.5, 0.8, and 0.9 are summarized in Table 2. An overestimate of AVHRR-derived cloud optical depth can be seen by comparing the retrieved optical depths in the last two columns of Table 2.

Table 2. Retrieval error of cloud optical depth t and cloud effective droplet size r_e from AVHRR and its comparison with that from DSSR for partial clouds.

Cloud cover fraction (r)	r_e=10 (μ m)	τ = 15	τ = 30	τ = 30 (DSSR)
0.5	15.4 (54%)	8.7 (42%)	12.9 (57%)	5.6 (81%)
0.8	12.1 (21%)	12.4 (17%)	21.7 (28%)	15.5 (48%)
0.9	11.0 (10%)	13.7 (9%)	25.9 (14%)	21.4 (29%)

These satellite-retrieved cloud optical depths and effective droplet sizes can be used as inputs to a one-dimensional radiative transfer model, in which the cloud is taken to be a homogeneous layer, to compute the downward solar irradiance DSSR* for a partially cloudy pixel.

Model simulations show that the computed DSSR using satellite-derived cloud optical depth for a partial cloud is underestimated (Figure 10). In this simulation, the SZA was 60°, cloud τ =15, and r_e = 10 μm. For a partial cloud cover over a snow surface DSSR* is smaller than DSSR by as much as 30%, and for a cloud cover fraction of 0.8, the differences are about 13% and 15% for a snow surface and a low albedo surface, respectively.

The downward solar irradiance estimated from the satellite-derived cloud optical depth under partly cloudy conditions is smaller than that computed from Eq. (1), i.e., $DSSR^*(\tau_{sat}) < DSSR(\tau_{surf})$. Thus, we have $\tau_{sat} > \tau_{surf}$, as shown in Figure 5. Here we retrieved the "effective" cloud optical depth τ_{surf} using the algorithm of Leontyeva and Stamnes (1994). So, for the same partial cloud cover, τ_{sat} is 1.3 to 2.3 times larger than τ_{surf}. From these simulations, we see that the presence of partial cloud cover might be an important reason for the overestimate of cloud optical depth derived from satellite measurements.

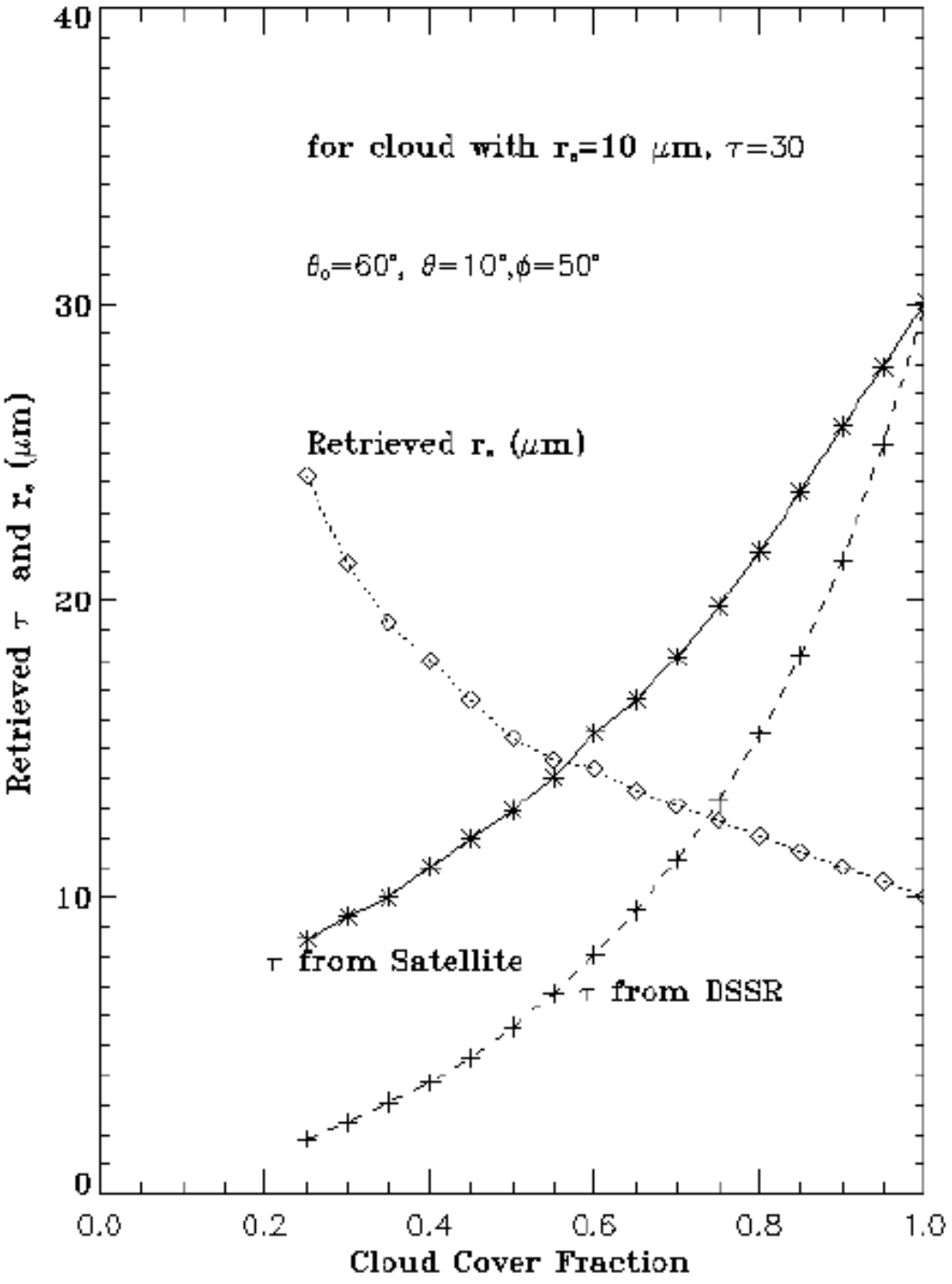

Figure 9. **Comparison of AVHRR-derived cloud effective droplet size and cloud optical depth from AVHRR and DSSR for a partial cloud.**

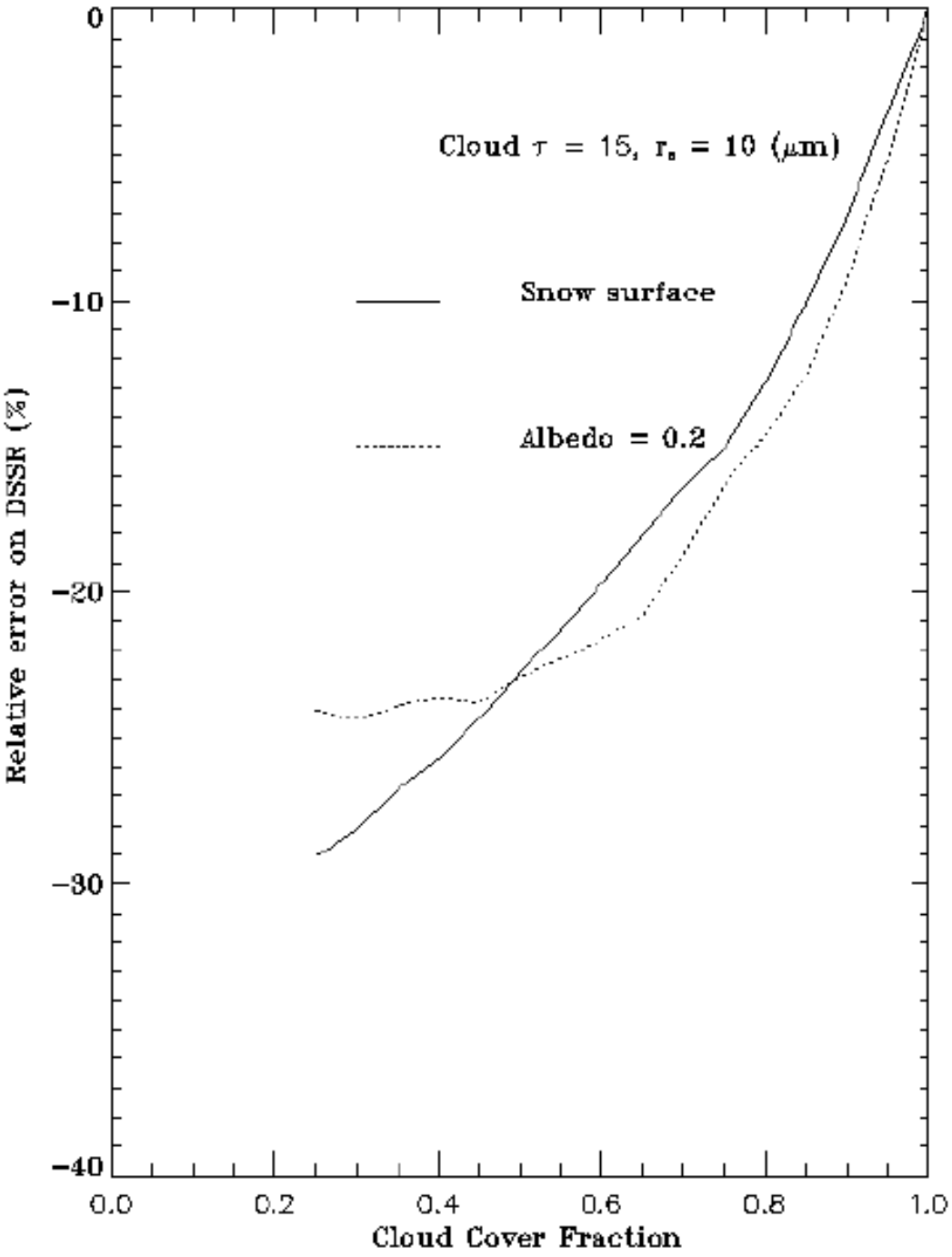

Figure 10. **Relative error of DSSR computed using AVHRR-derived optical depth for partial clouds.**

Discussion and Conclusion

Some data from the ARM NSA site were used to validate and improve the retrieval of cloud and surface properties. However, more validation with NSA/ARM data and collocated data from AVHRR and/or some other newly-deployed sensors will be obviously necessary to improve the cloud mask, derivation of ground "truth," and retrieval of cloud properties.

From our analyses we found the cloud optical depth derived from AVHRR is in better agreement with that derived from DSSR from June to August, but in the spring satellite retrieved cloud optical depth is 1 to 2 times larger than that derived from DSSR. Uncertainties analysis shows that the error due to cloud vertical inhomogeneity is 10% to 20%. Partial cloud cover will result in a higher τ_{sat} than τ_{surf}. As compared to summer, the cloud in the spring is thin and the cloud cover fraction is generally smaller; the significant overestimate of τ_{sat} in the spring but not in the summer may be partly due to the presence of partial cloud cover, however, the error due to cloud cover fraction is about 50%-80%. This implies that inaccurate representation of surface albedo and/or surface BRDF and incorrect representation of the scattering phase function for mixed-phased clouds and/or ice clouds may be other two important sources of uncertainty.

A preliminary comparison of AVHRR-derived albedo with that from surface observation shows that there is a good agreement in the spring, but not in the summer. This discrepancy mainly comes from the larger spatial coverage of AVHRR because it covers the coastal transition zone. Because the surface is more inhomogeneous in the summer than in the spring, the cloud cover is much higher than the spring, so the clear pixels observed by satellites may be a different area where surface observation is located. So, using the collocated surface observations with the overpass of AVHRR may give better results, but we have not done this in these preliminary results. Some points with much higher albedo from AVHRR in the summer are likely to be contaminated by clouds due to the error in the cloud mask because the algorithm for cloud masking we developed is for cloud over snow/ice surfaces. More improvements on cloud masks will be required.

Since the launch of NOAA-15, AVHRR makes use of a 1.6-μm channel instead of the 3.75-μm channel during daytime, so we lose information about the reflectance in the 3.75-μm channel. We may attempt using the 1.6-μm channel together with AVHRR channel 2 to retrieve τ and r_e, but the error in r_e is very large for clouds with τ <10 as shown in Figure 11. Since the optical depth of clouds is about 10 to 15 during summer in the Arctic, and a little smaller in the spring, it is difficult to use the 1.6-μm and AVHRR channel 2 on NOAA-K to retrieve effective droplet radius and optical depth simultaneously. However, use of the 1.6-μm channel instead of a visible channel and the 3.75-μm channel can produce more accurate values of τ and r_e over snow/ice surfaces for clouds if $\tau < 20$. The sensitivity of the TOA reflectance of clouds at 1.6 μm ($R_{1.6}$) with cloud optical depth decreases significantly when $\tau > 20$ (see lower panel of Figure 11). So simultaneous retrieval of r_e and τ may not be possible with an AVHRR sensor that switches channel 3 between 1.6 μm and 3.75 μm.

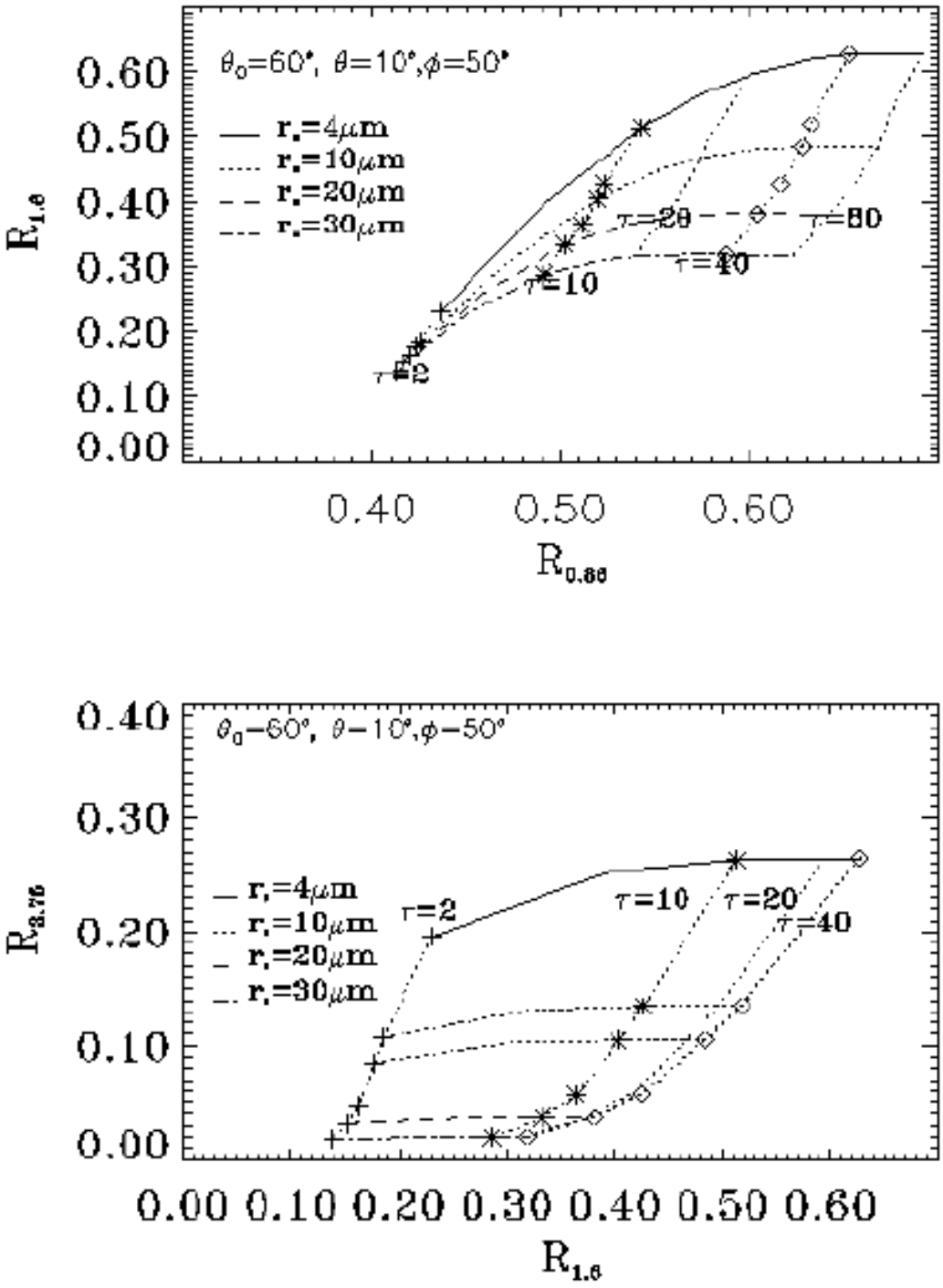

Figure 11. **TOA reflectance in the 1.6-μm channel versus reflectance at 0.86 μm (upper panel), and reflectance in the 3.75-μm channel versus that in the 1.6-μm channel (lower panel) for a variety of cloud optical depths and effective droplet sizes.**

A (horizontally and vertically) homogeneous cloud layer embedded in plane-parallel radiative transfer models constitutes the basis for most cloud retrieval algorithms. Since real clouds are inhomogeneous in both the vertical and horizontal directions (i.e., partial or broken cloud cover), there will be uncertainties in the retrieved cloud properties. These errors may lead to considerable uncertainties in estimated radiation budgets derived from satellite-retrieved cloud products including optical depth and effective droplet size. Here, we use a simple linear model to compute the downward surface solar irradiance in the presence of broken clouds, and to examine the uncertainties associated with partial cloud conditions. A better approach would be to use a rigorous three-dimensional radiative transfer model. Our investigation of partial cloud cover may appear to be an extreme representation of horizontally inhomogeneous clouds. Nevertheless, the resulting uncertainties in cloud retrievals and the differences between cloud optical depths derived from satellite data and from surface irradiance measurements give useful indications of the magnitude of retrieval errors associated with our inability to treat horizontal cloud inhomogeneity properly. In view of the large uncertainties, this is a very important issue that needs to be considered when using satellite-derived cloud products.

Acknowledgments

Data were obtained from the ARM Program, sponsored by the U.S. Department of Energy, Office of Science, Office of Biological and Environmental Research, Environmental Sciences Division. This research was supported by the ARM Program.

Corresponding Author

Xiaozhen Xiong, xiaozhen.xiong@noaa.gov, (301) 763-8247 X 50

References

Leontyeva, E., and K. Stamnes, 1994: Estimate of cloud optical thickness from ground-based measurements of incoming solar radiation in the Arctic. *J. Climate*, **7**, 566–578.

Lindsay R. W. and D. A. Rothrock, 1994: Arctic sea ice albedo from AVHRR. *J. Climate*, **7**, 1737-1749.

Perovich, D. K., T. C. Grenfell, B. Light, J. A. Richter-Menge, M. Sturm, W. B. Tucker III, H. Eicken, G. A. Maykut, and B. Elder, 1999: SHEBA: Snow and Ice Studies CD-ROM}. Obtainable from D. Perovich, CRREL, 72 Lyme Road, Hanover, New Hampshire, USA 03755.

Stephens, G. L., and C. M. R. Platt, 1987: Aircraft observations of the radiative and microphysical properties of stratocumulus and cumulus clouds fields. *J. Appl. Meteor*., **26**, 1243–1269.

Stroeve, J., Nolin, A., and K. Steffen, 1997: Comparison of AVHRR-derived and in situ surface albedo over the Greenland Ice Sheet. *Remote Sens. Environ*., **62**, 262–276.

Suttles, J. T., R. N. Green, P. Minnis, G. L. Smith, W. F. Staylor, B. A. Wielicki, I. J. Walker, D. F. Young, V. R. Taylor, and L. L. Stowe, 1988: Angular radiation models for earth-atmosphere system, volume 1, shortwave radiation, NASA Ref. Pub. 1184, National Aeronautics and Space Admin., Washington, D.C., 144 pp.

Xiong X., K. Stamnes, and D. Lubin, 2002: Retrieval of surface albedo over central Arctic Ocean and its validation with SHEBA data. *J. Appl. Meteor*. **41**, 413–425.